The Fifth JSME-KSME Fluids Engineering Conference
Nov. 17-21, 2002, Nagoya, Japan

Development of Genetic Algorithm Based Feedback Control System of Wall Turbulence

Takashi YOSHINO, Yuji SUZUKI, and Nobuhide KASAGI
Department of Mechanical Engineering, The University of Tokyo,
Hongo 7-3-1, Bunkyo-ku, Tokyo, 113-8656, Japan.
Takashi YOSHINO: yoshino@thtlab.t.u-tokyo.ac.jp

Abstract A prototype system for feedback control of wall turbulence is developed, and its performance is evaluated in a physical experiment. Arrayed micro hot-film sensors with a spanwise spacing of 1 mm are employed for the measurement of streamwise shear stress fluctuations, while arrayed magnetic actuators having 3 mm in diameter are used to introduce control input through wall deformation. The frequency response of the sensors and actuators is found to be sufficiently high for the flow conditions presently considered. A digital signal processor is employed to drive output voltage for actuators. It is found through the cross-correlation measurement between the wall shear stress and the wall deformation that the present control system has a time delay of 2.2 ms between sensing and actuation, which is smaller than the characteristic time scale of turbulence. When the driving voltage of the actuator is set to be proportional to the instantaneous wall shear stress, the wall-normal velocity fluctuations above the actuator is significantly increased, which indicates that the present actuators can introduce sufficiently large disturbances into the flow field. A preliminary feedback control experiment is also made using a genetic algorithms-based optimal control scheme. Although the number of generations is much smaller than that required for convergence, the Reynolds shear stress is decreased for several sets of control parameters among 50 trials.

Keywords: Feedback control, Genetic Algorithm, Electromagnetic Actuator, Hot-film sensor

1. INTRODUCTION

In the last decade, feedback control of wall turbulence was extensively pursued because of its potential of high control performance with small energy input [1][2][3]. In such a control system, the near-wall coherent structures, which are responsible for the turbulent transport mechanism, should be detected by sensors mounted on the wall, and selectively manipulated by the motion of actuators. Although the coherent structures have generally very small spatio-temporal scales, recent development of microelectromechanical systems (MEMS) technology has made it possible to fabricate flow sensors and mechanical actuators of sub-millimeter scale [4].

Recently, Endo et al. [5] carried out direct numerical simulation of turbulent channel flow, in which arrayed wall shear stress sensors and deformable actuators of finite spatial dimensions are assumed. They developed a practical control algorithm based on physical arguments on the near-wall coherent structures, and found that drag reduction of 12 % can be achieved by attenuating the near-wall streamwise vortices. Morimoto et al. [6] employed genetic algorithms to develop a simple feedback scheme based on the streamwise wall shear stress fluctuations, and obtained drag reduction of 12 % by using local wall blowing/suction. These findings encourage us to develop a feedback control system using distributed micro sensors and actuators in a laboratory experiment.

The objectives of the present study are to develop a prototype of feedback control system for wall turbulence with arrayed micro shear stress sensors and deformable actuators, and to evaluate their performance in a turbulent air channel flow.

2. FEEDBACK CONTROL SYSTEM OF WALL TURBULENCE

2.1 System configuration

Figure 1 shows a schematic diagram of feedback control system for wall turbulence. Several rows of arrayed micro sensors aligned in the spanwise direction are mounted flush on the wall, and arrays of actuators are placed in between. These devices are designed in such a way that the near-wall streamwise vortices are detected based on wall valuables and manipulated by the motion of actuators.

In the present study, hot-film sensors are employed for the measurement of the streamwise wall shear stress, while magnetic actuators are used to introduce control input into the flow field by wall deformation. Figure 2 shows a prototype control system, which consists of a single row of 8 hot-film sensors with a spanwise spac-

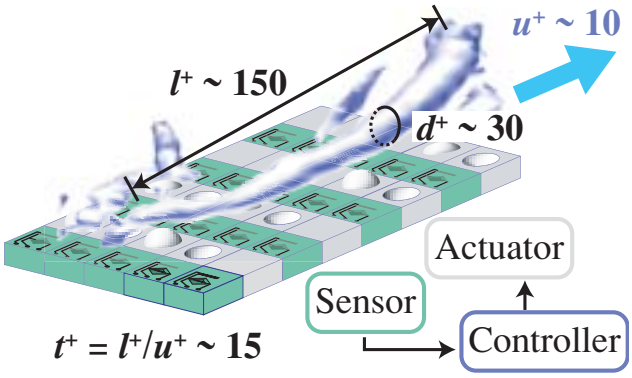

Fig. 1 Schematic diagram of active feedback control system for wall turbulence.

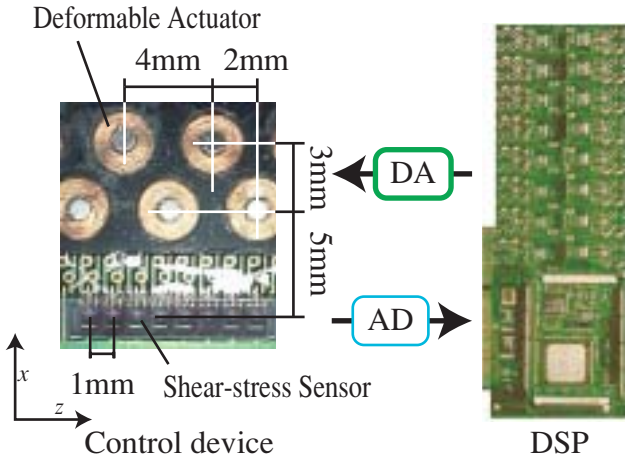

Fig. 2 Prototype system for wall turbulence control with arrayed sensors and actuators.

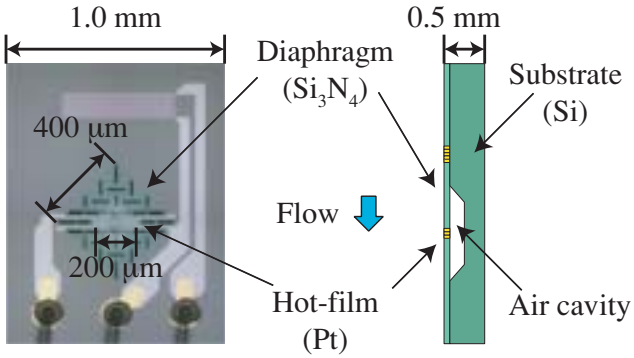

Fig. 3 Magnified view of micro hot-film shear stress sensor.

ing of 1 mm are used. Two staggered rows of arrayed actuators with a 4 mm spacing are located with a 2 mm offset in the spanwise direction, and thus five actuators are located with a 2 mm spanwise spacing. The spanwise spacings of the sensors and actuators are respectively about 10 and 20 wall units under the flow condition described later, which are in accordance with those of the DNS study by Endo et al. [5] and Morimoto et al. [6].

A digital signal processor (DSP) board (SMT-326, Sundance DSP Inc.) with 32 analog inputs/output channels is used as the controller of the present system. The output voltage of the constant temperature circuits for hot-film sensors are firstly digitized with the 16 bit AD converters. The control signals for the actuators are then computed with the DSP (C44, 60MFLOPS) and converted back to analog signal using the 16 bit DA converters. The present DSP system has an inherent time delay of 1.6 ms due to the data transfer and processing inside.

2.2 Micro wall shear stress sensor

Figure 3 shows a schematic of the micro shear stress sensor [7] used in the present study. A platinum thin-film heater is deposited on a Si_XN_Y diaphragm of 1 μm in thickness. In order to keep a sufficiently large electric resistance of the heater, a thin line of platinum is patterned zigzag in an area of 200×23 μm^2. An air cavity of 200 μm in depth is formed underneath the diaphragm (400×400 μm^2) for reducing thermal loss to the substrate. Another platinum resistor is made on the substrate and used for temperature compensation.

A turbulent air channel flow facility is employed for the experiments. The cross section is 50×500 mm^2, and the test section is located 4 m downstream from the inlet, where the flow is fully-developed. In our previous study [7], the frequency response of this sensor was evaluated and the power spectrum measured is compared with the DNS data [8] as shown in Fig. 4. It is found that the frequency response is flat up to only 40 Hz at Re_τ=300. The power spectrum is about 45 % of the DNS data at f^+=0.067. Since f^+=0.067 (t^+=15) corresponds to the duration of the near-wall streamwise vortices, the frequency response of the sensor should be high enough for our control purpose, although the response is imperfect.

Figure 5 shows the root-mean-square value of the streamwise wall shear stresses $\tau_{w\,rms}$ normalized by its mean value $\tau_{w\,mean}$. It is found in DNS studies [8][9] that $\tau_{w\,rms}/\tau_{w\,mean}$ is weakly dependent on the Reynolds number and equal to about 0.36-0.4. The present measurement data are decreased with increasing Reynolds number due to the imperfect response of the sensor. However, the error in $\tau_{w\,rms}/\tau_{w\,mean}$ is relatively small at Re_τ<400.

The spanwise two-point correlation of τ_w obtained with the arrayed sensors is shown in Fig. 6. The present data exhibit a negative peak at Δz^+~50, and are in good accordance with the DNS data. Therefore, the near-wall coherent structures, which are the target of the feedback control, can be well captured with the present wall shear stress sensors.

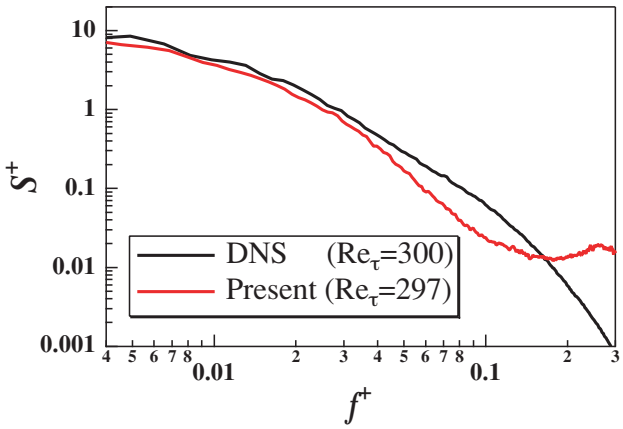

Fig. 4 Power spectra of the streamwise wall shear stress.

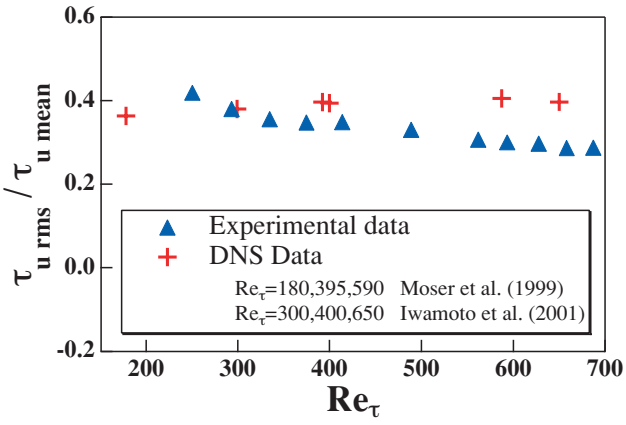

Fig. 5 Rms values of wall shear stress fluctuations.

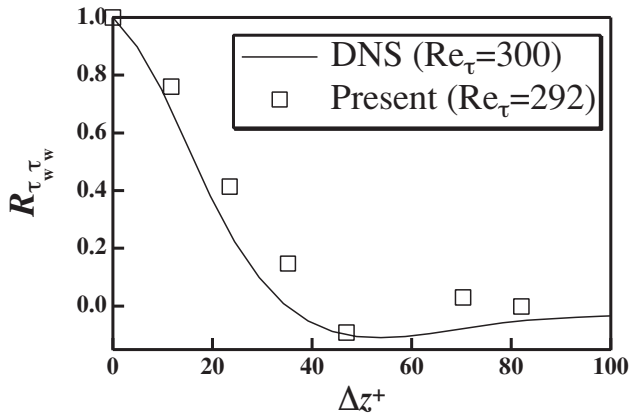

Fig. 6 Spanwise two-point correlations of the streamwise shear stress fluctuation.

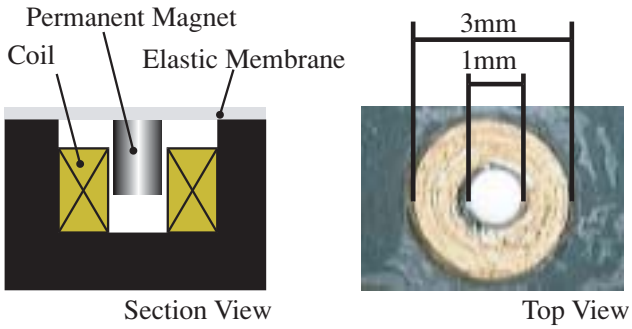

Fig. 7 Schematic of wall-deformation magnetic actuator.

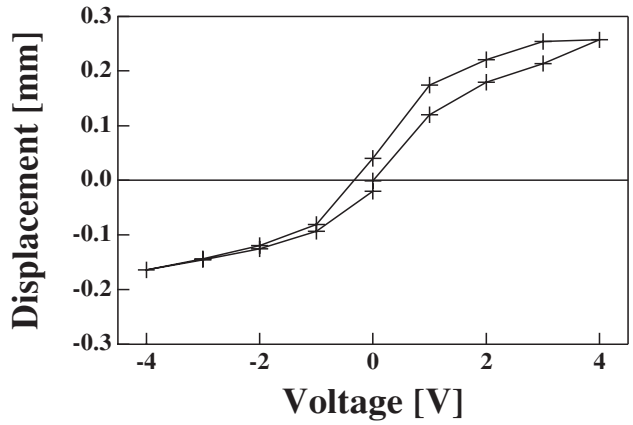

Fig. 8 Static response of wall-deformation magnetic actuator.

2.3 Deformable magnetic actuator

Figure 7 shows a schematic of deformable magnetic actuator. A silicone rubber sheet of 0.1 mm in thickness is used as an elastic membrane, and a rare-earth miniature permanent magnet of 1 mm in diameter is glued on its backside. A miniature copper coil (500 turns), of which outer diameter is 3 mm, is placed underneath the magnet. Figure 8 shows a static response of the actuator. The wall displacement is a nonlinear function of the voltage applied, and about 250 μm deformation is obtained with 4 V. Figure 9 shows the dynamic response of the actuator as a function of frequency of the sinusoidal driving voltage. Because the spring constant of the membrane is increased with increasing the deformation as shown in Fig. 8, the resonant frequency depends on the voltage amplitude; the resonant frequency is increased from 450 Hz to 600 Hz for 1-4 Vp-p signal. The time constant required for the experimental condition described later is about 7.5 ms, so that the frequency response of the actuator should be also sufficiently high.

3. EVALUATION OF PROTOTYPE CONTROL SYSTEM

3.1 Dynamic response of the system

The present prototype system is evaluated in the turbulent channel flow described above. The control system is placed at the bottom wall of the test section as shown in Fig. 10. The bulk mean velocity U_m is varied from 2.5 to 9.3 m/s, which corresponds to the Reynolds number Re_τ based on the wall friction velocity u_τ and the channel half-width from 250 to 800. When Re_τ=300 (U_m=3.0 m/s), one viscous wall and time unit correspond to 0.09 mm and 0.5 ms, respectively. At this flow condition, the mean diameter of the near-wall streamwise vortices is estimated to be 2.7 mm, while its characteristic time scale is 7.5 ms.

The dynamic response of the control system is evaluated by using a simple feedback scheme, in which the actuator driving signal E_A is set to be proportional to the instantaneous wall shear stress fluctuation, i.e.,

$$E_A = \alpha \tau_w' \qquad (1)$$

where the coefficient α is 88 V/Pa. The deformation of the actuator is measured with a laser displacement meter (Keyence Inc.,

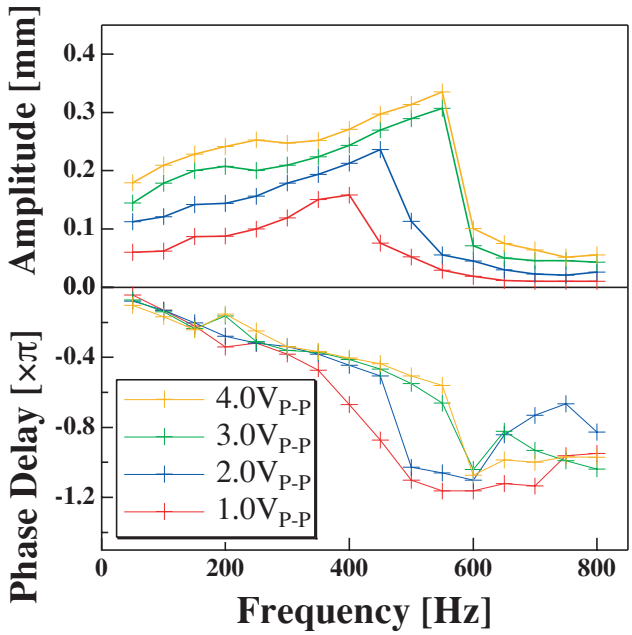

Fig. 9 Dynamic response of wall-deformation magnetic actuator.

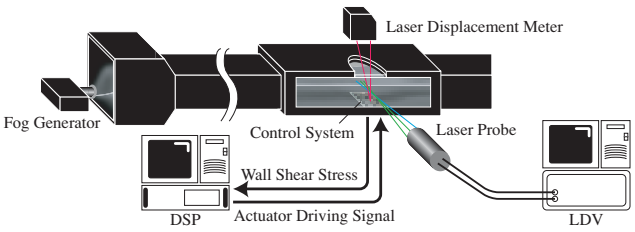

Fig. 10 Experimental setup for the flow and displacement measurement.

a)

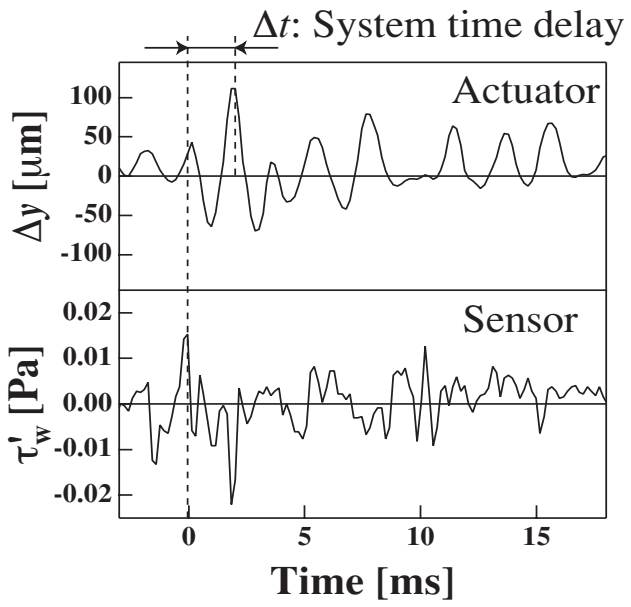

b)

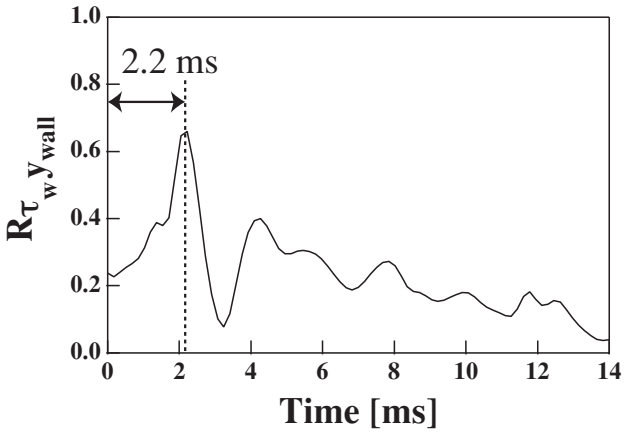

Fig. 11 System time delay measured with a simple feedback scheme, E_A=88 τ_w'. a) Time traces of actuator displacement and shear stress fluctuations, b) Cross correlation of the streamwise shear stress fluctuation and actuator displacement.

LC-2440), while the DSP continuously updates the driving voltage of the actuator. Figure 11(a) shows the time traces of the wall shear stress and of the actuator displacement. The cross correlation of these signals exhibits a marked peak at 2.2 ms (Fig. 11b), which corresponds to a time delay between sensing and actuation in the present control system. Therefore, most of the time delay is due to that of the DSP itself. Since mean traveling time of streamwise vortices from the sensors located upsteam to the actuators is estimated to be 2.8 ms, the present system still has a time margin of 0.6 ms.

In order to measure the streamwise and wall-normal velocity fluctuations near the wall, three-beam two-component LDV system (Dantec Dynamics Inc., 60X11) is employed. The focal length of the lens is 400 mm, and the measurement volume is about 190×190×5500 μm^2. Smoke particles of about 1 μm diameter, which are generated by the SAFEX® fog generator (Dantec Dynamics Inc., FOG 2010), are used as the flow tracers. Figure 12(a) shows the streamwise mean velocity profiles. Mean velocities for both unmanipulated and manipulated flows are in good agreement with the DNS result [8]. Figure 12(b) shows the root-mean-square velocity fluctuations. Although the streamwise component is unaltered by the motion of the actuator, the wall-normal velocity fluctuations are significantly increased at y^+=6. Since the magnitude of v^+_{rms} is much larger than that employed in previous DNS studies for active control, the present actuators should introduce enough disturbances into the flow field.

a)

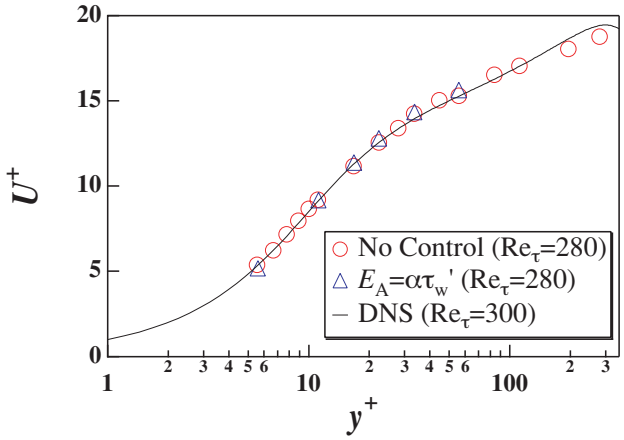

b)

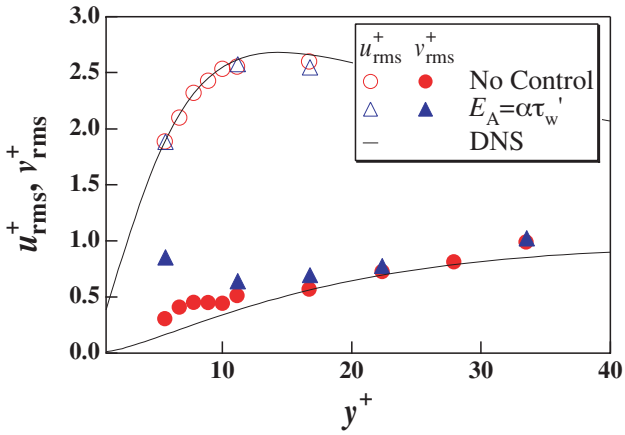

Fig. 12 Velocity measurement above the actuator in turbulent channel flow with a simple feedback scheme, E_A=88 τ_w'. a) streamwise mean velocity, b) Streamwise and wall-normal velocity fluctuations.

3.2 Genetic algorithm

An optimal control scheme based on genetic algorithm (GA) is employed in the present experiment. One of the deformable actuators and neighboring three wall shear stress sensors located upstream are employed in this preliminary experiment. The driving voltage of the actuator E_A is given by

$$E_A = \sum_{i=1}^{3} C_i \cdot E_i \qquad (2)$$

where E_i is the fluctuating component of the sensor output voltage. The control variable C_i is optimized in such a way that a cost func-

a)

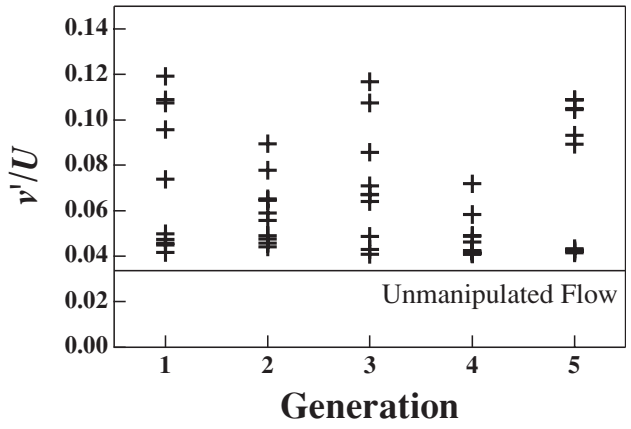

b)

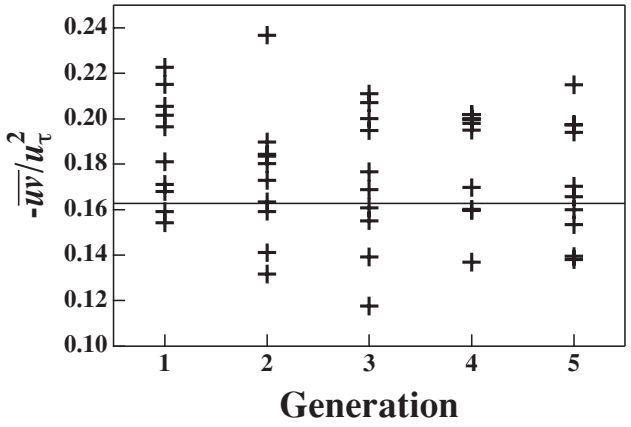

Fig. 13 LDV measurement at each generation when an optimal control scheme based on genetic algorithm is employed into a prototype system. a) wall-normal fluctuations at y^+=7.5, b) Reynolds stress at y^+=7.5.

tion

$$J = \int_t^{t+\Delta T} v'^2 \, dt \qquad (3)$$

is minimized. The wall-normal velocity fluctuation v' is measured with LDV as mentioned above. The measurement station is set to be y^+=7.5 above the actuator, and the integration time ΔT is chosen as 10 s (ΔT^+=2000). Hammond et al. [10] reported that, when the opposition control scheme is employed, the rms value of the wall-normal velocity fluctuations v_{rms} almost diminish at some elevation from the wall between the detection plane and the wall. Thus, when the cost function given by Eq. (3) is minimized, the present control scheme based on the wall shear stress is expected to be in accordance with the opposition control.

In our preliminary experiment, C_i in Eq. (2) is expressed with a binary-coded string with 5 bits. The population size, which is the number of individuals evaluated at each generation, is 10. In this experiment, the GA procedure was made off-line; v_{rms} was measured with LDV and the data are transferred to the control PC manually. Therefore, the number of generations is only five, which is much less than the value required for the convergence.

Figure 13(a) shows v_{rms} measured with LDV for the first five generations. Each data point represents control result for each gene. In all controlled cases, v_{rms} is larger than that of the unmanipulated flow, which is opposite to the objective of the present control. Figure 13(b) shows the Reynolds shear stress $-\overline{uv}/u_\tau^2$ for the control cases. Although v_{rms} is increased, $-\overline{uv}/u_\tau^2$ is widely distributed, and several data points give smaller $-\overline{uv}/u_\tau^2$ than that of the unmanipulated case.

4. CONCLUSIONS

The prototype of the feedback control system for wall turbulence is developed with arrayed micro hot-film sensors and arrayed wall-deformation magnetic actuators. The dynamic response of the sensors and actuators are found to be sufficiently high for the experimental condition employed. The time delay of the feedback loop of the present control system is estimated to be 2.2 ms, where the time delay of the DSP is the major cause. It is found in the LDV measurement that the present control system can introduce sufficiently large control input into the flow field. Preliminary control experiment is also made using a genetic algorithm-based optimal control scheme. Although v_{rms} is increased for all control cases, the Reynolds shear stress is decreased for several sets of control parameters among 50 trials.

The authors are grateful to Mr. S. Kamiunten in Yamatake Corp. for his corporation in manufacturing micro shear stress sensors. The authors also thank to Mr. Tsuda for his aid in his laboratory work. This work was supported through the Project for Organized Research Combination System by the Ministry of Education, Culture, Sports, Science and Technology of Japan (MEXT).

REFERENCES

[1] Moin, P., and Bewley, T., Appl. Mech. Rev., Vol. 47, S3-S13 (1994).
[2] Gad-el-hak, M., Appl. Mech. Rev., Vol. 49, 365-379 (1996).
[3] Kasagi, N., Int. J. Heat & Fluid Flow, Vol. 19, 128-134 (1998).
[4] Ho, C.-M., and Tai, Y.-C., ASME J. Fluids Eng. Vol. 118, 437-447 (1996).
[5] Endo, T., Kasagi, N., and Suzuki, Y., Int. J. Heat & Fluid Flow, Vol. 21, 568-575 (2000).
[6] Morimoto, S., Iwamoto, K., Suzuki, Y., and Kasagi, N., Bull. Am. Phys. Soc., Vol. 46, 185 (2001).
[7] Yoshino, Y., Suzuki, Y., Kasagi, N., and Kamiunten, S., 2nd Int. Symp. Turbulence and Shear Flow Phenomena, Stockholm, Vol. II, 153-158 (2001).
[8] Iwamoto, K., Suzuki, Y., and Kasagi, N., Int. J. Heat & Fluid Flow, Vol. 23, 678-689 (2002).
[9] Moser, R. D., Kim, J., and Mansour, N. N., Phys. Fluids, Vol. 11, 943-945 (1999).
[10] Hammond, E. P., Bewley, T. R., and Moin, P., Phys. Fluids, Vol. 10. 2421-2423 (1998).